3 Free surface flows

3.1 Introduction

We now move on to discuss potential flow with free surfaces. With only fixed (and known) boundaries we can find the potential whenever we can find the relevant conformal map. However, if there are *free* surfaces, these are unknown and we have to find them as part of the solution. We will discuss two scenarios where complex analysis and conformal mapping allows us to find analytic solutions.

3.2 Steady inviscid free surface flow

We now show how conformal mapping allows us to obtain steady, inviscid, incompressible, irrotational flows bounded by a combination of rigid walls and free surfaces. We recall that such flows may be described by a complex potential

$$w(z) = \phi + \mathrm{i}\psi, \tag{3.1}$$

where ϕ and ψ are the velocity potential and streamfunction, and the velocity components are then given by

$$u - \mathrm{i}v = \frac{\mathrm{d}w}{\mathrm{d}z}. \tag{3.2}$$

Any given fixed walls must be streamlines for the flow, so that $\psi = \operatorname{Im} w = \text{constant}$ there, and the velocity must be tangential to any such boundaries.

Any steady free surface must likewise be a streamline for the flow (this is the *kinematic* boundary condition). However, this is not enough information, because the location of the free surface is not known in advance. The additional condition to be imposed (the *dynamic* boundary condition) is that the external atmospheric pressure is assumed to be a known constant. (This condition must be generalised if surface tension is significant.) From Bernoulli's Theorem for a steady flow we have

$$p + \frac{1}{2}\rho|\boldsymbol{u}|^2 = p + \frac{1}{2}\rho\left|\frac{\mathrm{d}w}{\mathrm{d}z}\right|^2 = \text{constant} \tag{3.3}$$

and therefore, if p is constant, it follows that $|\mathrm{d}w/\mathrm{d}z|$ is constant, and this provides the additional information to locate the free surface.

The general solution technique will be demonstrated via an example.

Example: Teapot flow. A fluid layer of thickness h flows horizontally at speed U_∞ over a thin plate lying along the negative x-axis, before turning the corner at $x = 0$ and flowing back along the underside of the plate, as shown in Figure 3.1.

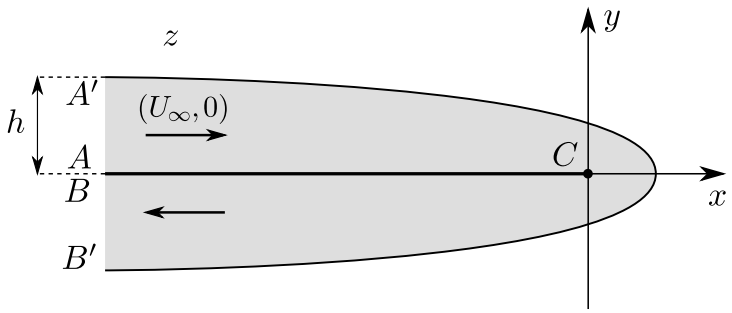

Figure 3.1: A model for flow round the spout of a teapot.

Solution. The plate ACB and the free surface $A'B'$ are both streamlines. The net flux is $U_\infty h$ so without loss of generality we set

$$\psi = 0 \text{ on } ACB, \qquad \psi = U_\infty h \text{ on } A'B'. \tag{3.4}$$

On the free surface we also have by Bernoulli's Theorem

$$|\boldsymbol{u}| = \text{constant} = U_\infty \text{ on } A'B'. \tag{3.5}$$

It is helpful to nondimensionalise by scaling z with h and w with $U_\infty h$. The resulting normalised problem is sketched in Figure 3.2, where we have also marked the "nose" N of the fluid.

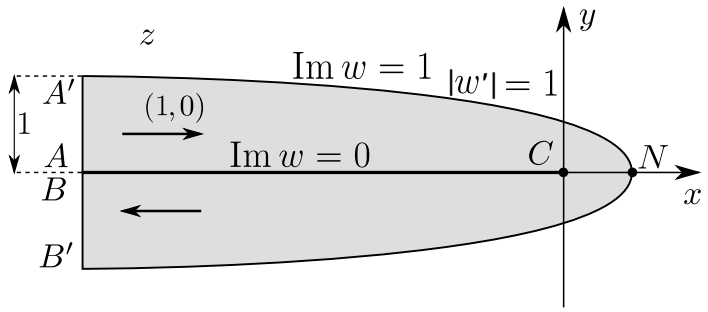

Figure 3.2: A normalised model for flow round the spout of a teapot.

Now we can view the complex potential as a conformal map $z \mapsto w(z)$ from the physical plane to the *potential plane*, and our first step is to examine what the image of the shaded fluid domain is in the w-plane. Recall that $w = \phi + \mathrm{i}\psi$. The fluid domain is bounded by curves on which $\psi = 0$ and $\psi = 1$, which are horizontal straight lines in the potential plane. At AA' we have $w \sim z$ and hence $\phi \sim x \to -\infty$. Similarly, at BB' we have $w \sim -z$ and hence $\phi \sim -x \to +\infty$. Finally, without loss of generality we can choose the origin for ϕ such that $w = 0$ at C. Then, since by symmetry $u = 0$ on CN, it follows that ϕ is constant on CN and therefore $\phi = 0$ at N. Therefore the fluid domain in the potential plane is as sketched in Figure 3.3, where $w = \mathrm{i}$ is the image of N.

Next we do the same for the *hodograph plane*, which is the image of the fluid domain under the mapping

$$z \mapsto w'(z) = \frac{\mathrm{d}w}{\mathrm{d}z} = u - \mathrm{i}v. \tag{3.6}$$

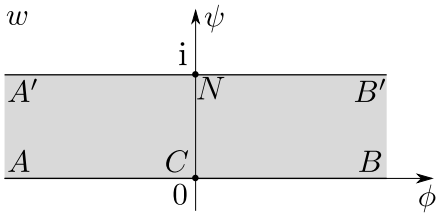

Figure 3.3: The potential plane for the teapot flow.

On the plate, the normal velocity must be zero, i.e. $v = 0$ on $y = 0$, so the streamline ACB is mapped to the u-axis. At C, the fluid turns through an angle $2\pi > \pi$, so the velocity will be infinite at the corner. Therefore u increases from 1 at A to $+\infty$ at C, then on the underside of the plate increases from $-\infty$ at C to -1 at B. Since $|w'| = 1$ on the free surface, the curve $A'B'$ is mapped to a portion of the unit circle in the hodograph plane. We infer from Figure 3.2 that $v < 0$ everywhere, with $v \to 0$ at A and A', while $v = -1$ and $u = 0$ at the nose N. Therefore the flow in the hodograph plane is as shown in Figure 3.4.

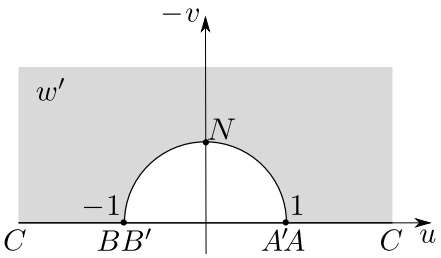

Figure 3.4: The hodograph plane for the teapot flow.

Now we map both the potential and the hodograph planes to *the same region* in an auxillary ζ plane. Note that

$$\zeta = \mathrm{e}^{\pi w} \tag{3.7}$$

maps the strip $0 < \operatorname{Im} w < 1$ to the upper half ζ-plane, while $A \mapsto 0$, $B \mapsto \infty$, $C \mapsto 1$ and $N \mapsto -1$, as shown in Figure 3.5.

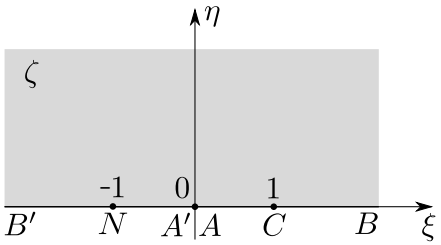

Figure 3.5: The potential plane for the teapot flow is mapped to the upper half-plane by the mapping $\zeta = \mathrm{e}^{\pi w}$.

Now, the mapping

$$\zeta = \left(\frac{w' - 1}{w' + 1)} \right)^2 \tag{3.8}$$

maps the hodograph plane onto the upper half ζ-plane, *and maps the points A, B, C, N to the same points on the real ζ-axis.* Once the locations of three points on the boundary have been fixed, the conformal map from any domain onto the upper half-plane is unique. Therefore, the complex potential and its derivative must satisfy the relation

$$e^{\pi w} = \zeta = \left(\frac{w'-1}{w'+1}\right)^2, \tag{3.9}$$

i.e. we get a differential equation for $w(z)$!

By rearranging (3.9) we get a separable differential equation

$$w' = \frac{1+e^{\pi w/2}}{1-e^{\pi w/2}} = -\coth\left(\frac{\pi w}{4}\right), \tag{3.10}$$

and integration leads to

$$\frac{4}{\pi}\log\cosh\left(\frac{\pi w}{4}\right) = -z, \tag{3.11}$$

where we have applied the boundary condition $w = 0$ when $z = 0$. Thus the complex potential $w(z)$ is given by

$$\cosh\left(\frac{\pi w}{4}\right) = \mathrm{e}^{-\pi z/4}, \tag{3.12}$$

or (by squaring both sides)

$$1 + \cosh\left(\frac{\pi w}{2}\right) = 2\mathrm{e}^{-\pi z/2}. \tag{3.13}$$

The free streamline is given by $\psi = 1$, i.e $w = \phi + \mathrm{i}$ with $\phi \in (-\infty, \infty)$, so that

$$2\mathrm{e}^{-\pi z/2} = 1 + \cosh\left(\frac{\pi\phi}{2} + \frac{\mathrm{i}\pi}{2}\right) = 1 + \mathrm{i}\sinh\left(\frac{\pi\phi}{2}\right). \tag{3.14}$$

By taking the real part of both sides, we deduce that the position of the free surface is given by the equation

$$\mathrm{e}^{-\pi x/2}\cos\left(\frac{\pi y}{2}\right) = \frac{1}{2}. \tag{3.15}$$

In particular, the film thickness at the nose $y = 0$ is given by $x = (2\log 2)/\pi \approx 0.441$: this is known as the *thinning factor*.

Example: Flow out of a slot. Fluid occupies the upper half-plane $y > 0$ above a wall at $y = 0$. There is a gap in the wall in the interval $x \in (-a, a)$, through which the fluid flows into $y < 0$ as a jet between two free surfaces. The free surfaces detach tangentially from the edges $x = \pm a$ of the slot (this *Kutta condition* ensures that the velocity is finite at these points). The jet thickness far downstream is $2Qa$, where the *contraction ratio* Q is to be found. The set-up is sketched in Figure 3.6.

If $p \to p_\infty$ and $\boldsymbol{u} \to \mathbf{0}$ as $y \to \infty$, then by Bernoulli's equation we have

$$p + \frac{1}{2}\rho|\mathbf{u}|^2 = p_\infty. \tag{3.16}$$

On the other hand, on the free surfaces BC and DC' we have $p = p_{\mathrm{atm}}$, the atmospheric pressure. Therefore on the free surface we have $|\boldsymbol{u}| = U_\infty$, where U_∞ is the speed of the uniform flow at CC' and is given by

$$\frac{1}{2}\rho U_\infty^2 = p_\infty - p_{\mathrm{atm}}. \tag{3.17}$$

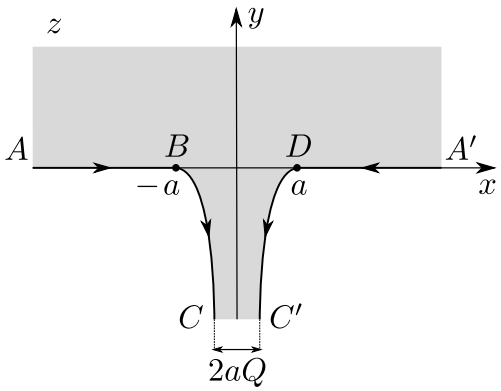

Figure 3.6: Flow out of a slot.

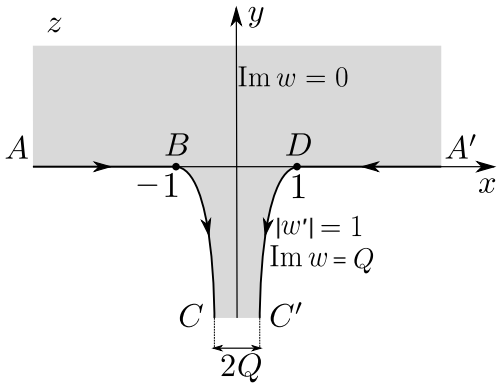

Figure 3.7: Normalised problem for flow out of a slot.

We nondimensionalise the problem by scaling z with a and w with $U_\infty a$; the resulting normalised problem is sketched in Figure 3.7. By symmetry, the y-axis is a streamline, which we choose to be $\psi = 0$. Then, given that the net flux in the jet is $2Q$, we have $\psi = Q$ on the streamline $A'DC'$ and $\psi = -Q$ on ABC. At infinity in the upper half-plane $\psi \sim Q - 2Q\theta/\pi$, where $\theta = \arg z$, which corresponds to

$$w(z) \sim -\frac{2Q}{\pi} \log z + Q \quad \text{as } z \to \infty \text{ with } \operatorname{Im} z > 0. \tag{3.18}$$

This is the complex potential due to a *point sink* of strength $4Q$, and implies that $\phi \to -\infty$ as $z \to \infty$ in the upper half-plane. At CC' we have $\phi \sim -U_\infty y$ and therefore $\phi \to \infty$ there. The potential plane is therefore as shown in Figure 3.8.

For the hodograph plane, note that the velocity tends to zero at infinity in the upper half-plane, so $w' \to 0$ at AA'. The free surfaces BC and DC' are mapped to arcs of the unit circle, with $\{u = 1, v = 0\}$ at B, $\{u = 0, v = -1\}$ at CC' and $\{u = -1, v = 0\}$ at D. The walls AB and $A'D$ are mapped to the straight lines $v = 0$, with $u \to 0$ at A and A', $u = 1$ at B and $u = -1$ at D. Therefore the hodograph plane is as shown in Figure 3.9.

The map

$$\zeta = -\left(\frac{1 - w'}{1 + w'}\right)^2 \tag{3.19}$$

takes the hodograph plane to the upper half-plane shown in Figure 3.10.

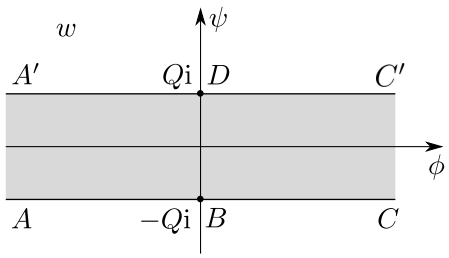

Figure 3.8: The potential plane for flow out of a slot.

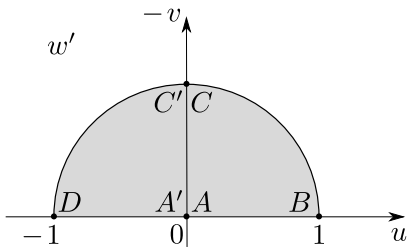

Figure 3.9: Hodograph plane for flow out of a slot.

The map

$$\zeta_1 = \mathrm{i}\,\mathrm{e}^{\pi w/2Q} \tag{3.20}$$

maps the potential plane to the upper half-plane shown in Figure 3.11, but the points along the real axis are in the wrong order! We can rearrange the points and thus map the ζ_1-plane onto the ζ-plane with the Möbius mapping

$$\zeta = \frac{\zeta_1 - 1}{\zeta_1 + 1} \tag{3.21}$$

to give

$$\left(\frac{1-w'}{1+w'}\right)^2 = \frac{1-\mathrm{i}\,\mathrm{e}^{\pi w/2Q}}{1+\mathrm{i}\,\mathrm{e}^{\pi w/2Q}}. \tag{3.22}$$

This is possible, but complicated, to solve.

If we just want the free surface shape there is a short cut to a parametric form. On the free surface we know that $|w'| = 1$ and therefore we can write

$$w' = \mathrm{e}^{-\mathrm{i}\theta}, \tag{3.23}$$

where θ is the angle the surface makes with the x-axis; $-\theta$ is the polar angle in the $(u, -v)$ hodograph plane. On BC we have $-\pi/2 < \theta < 0$, while on $C'D$ we have $-\pi < \theta < -\pi/2$, as can be seen in Figure 3.9.

Substituting (3.23) into (3.22), we find

$$\frac{1-\mathrm{i}\,\mathrm{e}^{\pi w/2Q}}{1+\mathrm{i}\,\mathrm{e}^{\pi w/2Q}} = \left(\frac{1-\mathrm{e}^{-\mathrm{i}\theta}}{1+\mathrm{e}^{-\mathrm{i}\theta}}\right)^2 = -\tan^2(\theta/2)\,, \tag{3.24}$$

which we invert to get

$$\mathrm{i}\,\mathrm{e}^{\pi w/2Q} = \frac{1+\tan^2(\theta/2)}{1-\tan^2(\theta/2)} = \sec\theta. \tag{3.25}$$

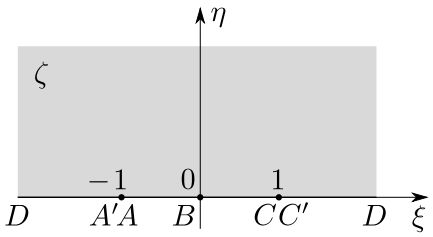

Figure 3.10: The hodograph plane for flow out of a slot is mapped to this upper half-plane by the mapping (3.19).

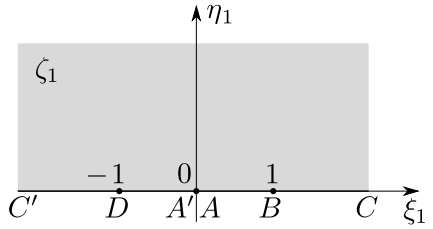

Figure 3.11: The potential plane for flow out of a slot is mapped to this upper half-plane by the mapping $\zeta_1 = \mathrm{i}\,\mathrm{e}^{\pi w/2Q}$.

Now differentiate both sides with respect to θ,

$$\frac{\mathrm{i}\pi}{2Q}\,\mathrm{e}^{\pi w/2Q}\,\frac{\mathrm{d}w}{\mathrm{d}z}\,\frac{\mathrm{d}z}{\mathrm{d}\theta} = \sec\theta\tan\theta, \tag{3.26}$$

and substitute w' and $\mathrm{e}^{\pi w/2Q}$ from (3.23) and (3.25) to find that

$$\frac{\mathrm{d}z}{\mathrm{d}\theta} = \frac{2Q}{\pi}\,\mathrm{e}^{\mathrm{i}\theta}\tan\theta. \tag{3.27}$$

Integration of this ODE gives a parametric equation $z(\theta)$ for the position of the free surface.

Taking real and imaginary parts, we get

$$\frac{\mathrm{d}x}{\mathrm{d}\theta} = \frac{2Q}{\pi}\,\sin\theta, \qquad\qquad \frac{\mathrm{d}y}{\mathrm{d}\theta} = \frac{2Q}{\pi}\,\sin\theta\tan\theta, \tag{3.28}$$

and integration with respect to θ gives

$$x = \text{const} - \frac{2Q}{\pi}\,\cos\theta, \qquad y = \text{const} + \frac{2Q}{\pi}\big(\log|\sec\theta + \tan\theta| - \sin\theta\big). \tag{3.29}$$

Considering the free surface BC, for example, we fix the constants by setting $x = -1$ and $y = 0$ at $\theta = 0$, resulting in

$$x = -1 + \frac{2Q}{\pi}\big(1 - \cos\theta\big), \qquad y = \frac{2Q}{\pi}\big(\log|\sec\theta + \tan\theta| - \sin\theta\big). \tag{3.30}$$

At C we have $\theta \to -\pi/2$, which gives $y \to -\infty$ and

$$x \to -1 + \frac{2Q}{\pi} = -Q. \tag{3.31}$$

Hence we can solve for the contraction ratio:

$$Q = \frac{\pi}{\pi + 2} \approx 0.611, \tag{3.32}$$

which agrees with experiments. The resulting jet shape is plotted in Figure 3.12.

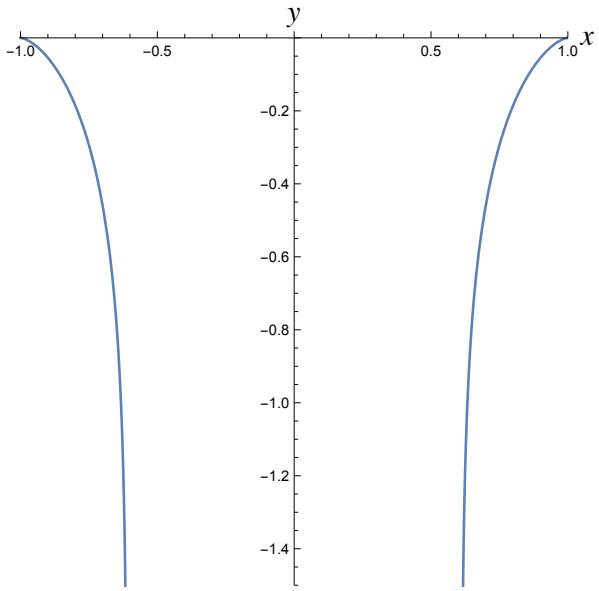

Figure 3.12: The jet shape given parametrically by (3.30) and (3.32).

3.3 Flow in porous media

Background

Darcy's Law was formulated by nineteenth-century French hydraulic engineer Henry Darcy to describe the flow of a viscous liquid through a porous medium, e.g. the flow of groundwater through rock or the flow of air through a filter. Darcy's Law relates the fluid velocity $\boldsymbol{u}$ to the pressure p through the relation

$$\boldsymbol{u} = -\frac{k}{\mu}\,\boldsymbol{\nabla} p, \tag{3.33}$$

where μ is the *viscosity* of the fluid and k is the *permeability* of the porous matrix. If the fluid is incompressible, then we also have $\boldsymbol{\nabla}\cdot\boldsymbol{u} = 0$ and thus, provided the medium is uniform (so that μ and k are constant), the pressure satisfies *Laplace's equation*

$$\nabla^2 p = 0. \tag{3.34}$$

The same equations also arise in *Hele-Shaw flow*, in which a viscous fluid is forced between two parallel plates, as shown in Figure 3.13. In this case, the permeability is given by $k = h^2/12$, where h is the thicknesss of the gap between the two plates.

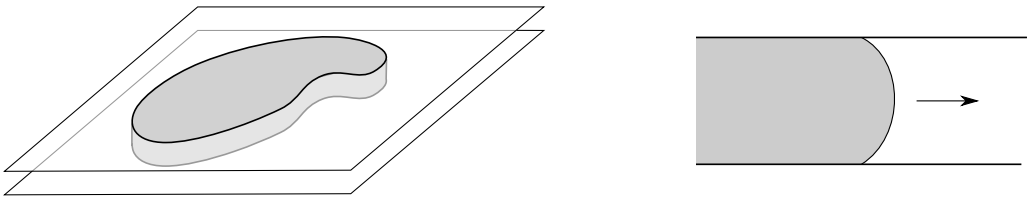

Figure 3.13: Hele-Shaw flow between two parallel plates; the right-hand diagram shows the cross-section.

Hele-Shaw flow (or two-dimensional porous medium flow) therefore provides an analogue of two-dimensional inviscid irrotational flow. However, if there are any free boundaries, then the boundary conditions there are different: a constant pressure is equivalent to $\phi =$ constant (where ϕ is the velocity potential) which is not at all similar to the Bernoulli condition relevant to inviscid flow.

We henceforth take $k/\mu = 1$ (via nondimensionalisation) and focus on two-dimensional flow, so that

$$\boldsymbol{u} = (u, v) = -\boldsymbol{\nabla} p = \boldsymbol{\nabla}\phi \tag{3.35}$$

in the fluid, where $\phi = p_{\text{atm}} - p$ is the velocity potential. At any free surface we have $p = p_{\text{atm}}$, the external atmospheric pressure, and hence

$$\phi = 0 \quad \text{at free boundary.} \tag{3.36}$$

We also have the *kinematic* boundary condition that the normal velocity $\boldsymbol{u}\cdot\boldsymbol{n}$ of the fluid must equal the normal velocity v_n of the boundary, i.e.

$$\frac{\partial\phi}{\partial n} = -\frac{\partial p}{\partial n} = v_n \quad \text{at free boundary.} \tag{3.37}$$

A convenient way to write this is to note that $p(x, y, t) = 0$ on the interface, and hence by differentiating with respect to t:

$$\frac{\mathrm{d}p}{\mathrm{d}t} = \frac{\partial p}{\partial t} + \boldsymbol{u}\cdot\boldsymbol{\nabla} p = \frac{\partial p}{\partial t} - \boldsymbol{\nabla} p\cdot\boldsymbol{\nabla} p = 0. \tag{3.38}$$

Thus the free boundary conditions are

$$\phi = 0, \quad \frac{\partial\phi}{\partial t} + |\boldsymbol{\nabla}\phi|^2 = 0 \quad \text{at free boundary.} \tag{3.39}$$

Again we note that these are quite different from the conditions at a free boundary in inviscid potential flow.

Canonical injection problem

A canonical problem is injection or suction from a point source/sink into a two-dimensional porous medium or Hele-Shaw cell, as shown in Figure 3.14. Given the strength Q of the

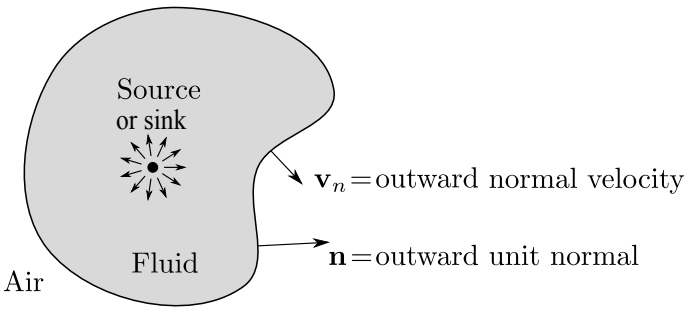

Figure 3.14: Schematic of injection into a Hele-Shaw cell.

source/sink and the initial shape $D(0)$ of the fluid domain at time $t = 0$, our aim is to

determine how the fluid domain $D(t)$ evolves as t increases. Without loss of generality, we can assume that the source/sink is at the origin. Then the required singularity is

$$\phi \sim \frac{Q}{2\pi} \log|z| \quad \text{as } z \to 0, \tag{3.40}$$

where $Q > 0$ is a source and $Q < 0$ is a sink. The conditions on the free boundary are given by equation (3.39), and the whole problem for ϕ is sketched in Figure 3.15.

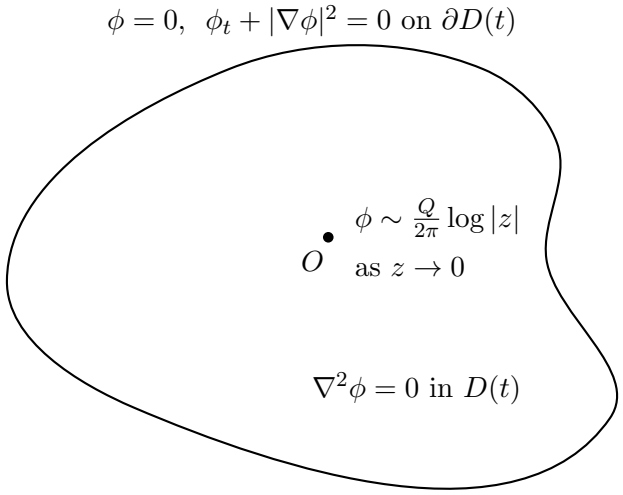

Figure 3.15: Canonical injection/suction free boundary problem.

As ϕ is a velocity potential we have a complex potential $w(z,t) = \phi + \mathrm{i}\psi$, which is a holomorphic function of z inside $D(t)$ except for a singularity at $z = 0$, with

$$w(z,t) \sim \frac{Q}{2\pi} \log z \quad \text{as } z \to 0. \tag{3.41}$$

Clearly there is a branch point at $z = 0$, which reflects the fact that the streamfunction ψ increases by Q on a circuit of O. The velocity, given by $u - \mathrm{i}v = \partial w/\partial z$ has a pole at $z = 0$ but is single-valued. The boundary conditions (3.39 imply that

$$\operatorname{Re} w = 0, \qquad \operatorname{Re}\left[\frac{\partial w}{\partial t}\right] + \left|\frac{\mathrm{d}w}{\mathrm{d}z}\right|^2 = 0 \quad \text{on } \partial D(t). \tag{3.42}$$

Now suppose that $D(t)$ is the image of the unit disc $|\zeta| < 1$ under a time-dependent conformal map $\zeta \mapsto z = F(\zeta, t)$, as shown schematically in Figure 3.16. By the Riemann Mapping Theorem, there are three real degrees of freedom in the resulting map, so we can choose also to map the origin to itself, so that $F(0,t) \equiv 0$.

We write the complex potential in the ζ-plane as

$$W(\zeta, t) = w\big(F(\zeta,t), t\big). \tag{3.43}$$

In the ζ-plane $W(\zeta,t)$ is a holomorphic function whose real part vanishes on $|\zeta| = 1$ and with a logarithmic singularity at $\zeta = 0$. We see that the appropriate function is

$$W(\zeta,t) = \frac{Q}{2\pi} \log\zeta. \tag{3.44}$$

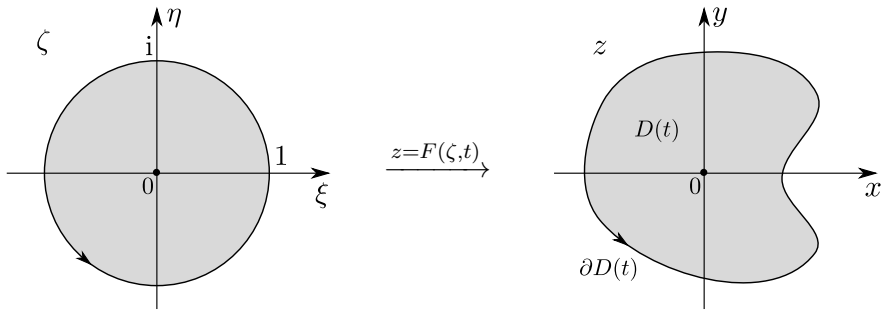

Figure 3.16: The fluid region $D(t)$ is the image of the unit disc $|\zeta| < 1$ under a time-dependent conformal map $z = F(\zeta, t)$.

It remains to impose the boundary condition (3.42). By differentiating (3.43) with respect to ζ and t we have

$$\frac{\partial W}{\partial \zeta} = \frac{\partial w}{\partial z}\frac{\partial F}{\partial \zeta}, \qquad \frac{\partial W}{\partial t} = \frac{\partial w}{\partial t} + \frac{\partial w}{\partial z}\frac{\partial F}{\partial t}, \tag{3.45}$$

and hence

$$\frac{\partial w}{\partial t} = \frac{\partial W}{\partial t} - \frac{\partial W}{\partial \zeta}\frac{\partial F}{\partial t}\Big/\frac{\partial F}{\partial \zeta} \tag{3.46}$$

Therefore the boundary condition (3.42) is equivalent to

$$\mathrm{Re}\left[\frac{\partial W}{\partial t} - \frac{\partial W}{\partial \zeta}\frac{\partial F}{\partial t}\Big/\frac{\partial F}{\partial \zeta}\right] + \left|\frac{\partial W}{\partial \zeta}\right|^2 \Big/ \left|\frac{\partial F}{\partial \zeta}\right|^2 . \tag{3.47}$$

Now we just substitute for $W(\zeta, t)$ from (3.44), assuming that Q is constant, so that $\partial W/\partial t = 0$:

$$\mathrm{Re}\left[-\frac{Q}{2\pi\zeta}\,\frac{\partial F}{\partial t}\Big/\frac{\partial F}{\partial \zeta}\right] + \frac{Q^2}{4\pi^2|\zeta|^2}\Big/\left|\frac{\partial F}{\partial \zeta}\right|^2 = 0. \tag{3.48}$$

On the free boundary $|\zeta| = 1$ this tidies up to

$$\mathrm{Re}\left[\zeta\,\frac{\partial F}{\partial \zeta}\,\overline{\frac{\partial F}{\partial t}}\right] = \frac{Q}{2\pi}, \tag{3.49}$$

which is known as the *Polubarinova-Galin equation*.

The initial shape of the fluid domain $D(0)$ in principle determines $F(\zeta, 0)$. If we can solve equation (3.49) for $F(\zeta, t)$, then the shape of the fluid domain $D(t)$ for $t > 0$ is given by the image of the unit disc under the map $z = F(\zeta, t)$. There is no general method to solve equation (3.49), but a large number of exact solutions do exist, as the following Theorem (proved on the problem sheet) shows.

Theorem. If $F(\zeta, 0)$ is a polynomial of degree n, conformal and one-to-one for $|\zeta| < 1$, then $F(\zeta, t)$ remains a polynomial of degree n for $t > 0$; moreover the (time-dependent) coefficients of this polynomial satisfy a set of $n + 1$ ODEs.

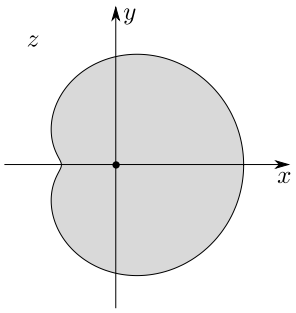

$$\begin{aligned} x &= a_{10}\cos\theta + a_{20}\cos 2\theta, \\ y &= a_{10}\sin\theta + a_{20}\sin 2\theta. \end{aligned}$$

Figure 3.17: A limaçon.

Example. Suppose $F(\zeta, 0) = a_{10}\zeta + a_{20}\zeta^2$, where a_{10}, a_{20} are real and positive, and $a_{10} > 2a_{20}$ (so that $F' \neq 0$ on the unit disc). Find the evolution under a source/sink at the origin.

Solution. The initial shape is called a *limaçon*, as illustrated in Figure 3.17.

We try

$$F(\zeta, t) = a_1(t)\zeta + a_2(t)\zeta^2, \tag{3.50}$$

where a_1, a_2 are real. Then substitution into the evolution equation (3.49) leads to

$$\mathrm{Re}\left[\zeta(a_1 + 2a_2\zeta)(\dot{a}_1\overline{\zeta} + \dot{a}_2(t)\overline{\zeta}^2)\right] = \frac{Q}{2\pi} \quad \text{on } |\zeta| = 1. \tag{3.51}$$

Since $\zeta\overline{\zeta} = 1$ this is equivalent to

$$\mathrm{Re}\left[a_1\dot{a}_1 + 2a_2\dot{a}_2 + 2a_2\dot{a}_1\zeta + a_1\dot{a}_2\overline{\zeta}\right] = \frac{Q}{2\pi}, \tag{3.52}$$

which must be true for all $|\zeta| = 1$, and hence we obtain two ODEs for the coefficients a_1 and a_2:

$$a_1\dot{a}_1 + 2a_2\dot{a}_2 = \frac{Q}{2\pi}, \qquad\qquad 2a_2\dot{a}_1 + a_1\dot{a}_2 = 0. \tag{3.53}$$

The first equation (3.53a) is an exact differential which we can integrate directly to give

$$\frac{1}{2}\left(a_1^2 + 2a_2^2\right) = \frac{Qt}{2\pi} + \frac{1}{2}\left(a_{10}^2 + 2a_{20}^2\right), \tag{3.54}$$

which represents net mass conservation. Multiplying (3.53b) by a_1 turns that into an exact differential, which we can integrate to give

$$a_1^2 a_2 = a_{10}^2 a_{20}. \tag{3.55}$$

Equations (3.54) and (3.55) determine $a_1(t)$ and $a_2(t)$ for $t > 0$. To get explicit formulae involves messy solution of a cubic. However, we can deduce the qualitative behaviour by eliminating $\dot{a}_2$ from (3.53) to get

$$a_1\dot{a}_1\left(1 - \frac{4a_2^2}{a_1^2}\right) = \frac{Q}{2\pi}. \tag{3.56}$$

First consider the case of injection, with $Q > 0$. Since we assumed that $a_1 > 2a_2$ initially, $\dot{a}_1 > 0$ initially. But (3.55) implies that, if a_1 increases, then a_2 decreases so that $a_1 > 2a_2$ always. Thus when $Q > 0$, a_1 increases with t while a_2 decreases, and $D(t)$ approaches a large circle. However, if $Q < 0$ (suction), then a_1 decreases and a_2 increases, until we get to a time when $a_1 = 2a_2$ and the map ceases to be conformal at $\zeta = -1$. At this point there is a *cusp* on the boundary (which is then a *cardioid*), and the solution ceases to exist. The evolution for positive and negative values of Q is shown in Figure 3.18.

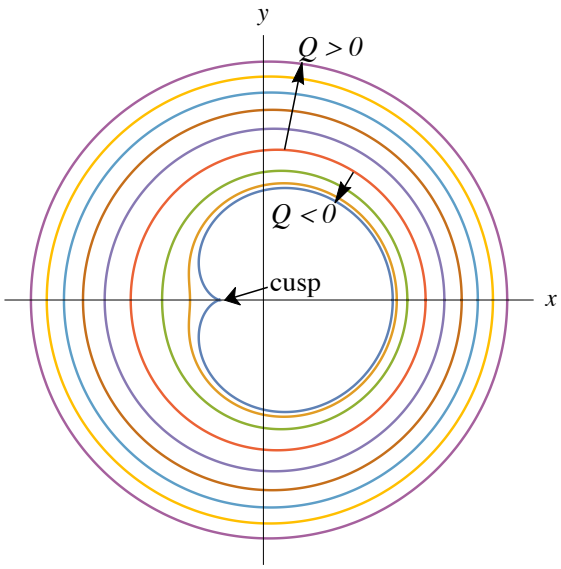

Figure 3.18: A limaçon evolving under Hele-Shaw flow due to a source/sink at the origin.

This example shows that for the case of suction, with $Q < 0$, the free surface may develop a cusp in finite time. In fact the situation is much worse than this. The suction problem is *ill posed*, in that an arbitrarily small perturbation to the initial boundary $\partial D(0)$ may lead to an arbitrarily large change in the boundary $\partial D(t)$ after an arbitrarily small time t. In reality, such pathalogical behaviour is prevented by physical effects not included in our model, for example surface tension.